

Linear and Nonlinear Optical Properties of Tris-cyclometalated Phenylpyridine Ir(III) Complexes Incorporating π -Conjugated Substituents

Moussa Zaarour,[†] Anu Singh,[‡] Camille Latouche,[†] J. A. Gareth Williams,[§] Isabelle Ledoux-Rak,[‡] Joseph Zyss,[‡] Abdou Boucekkine,[†] Hubert Le Bozec,[†] Véronique Guerschais,^{*,†} Claudia Dragonetti,^{||} Alessia Colombo,^{||} Dominique Roberto,^{*,||} and Adriana Valore^{||}

[†]Institut des Sciences Chimiques de Rennes, UMR 6226 CNRS-Université de Rennes 1, Campus de Beaulieu, 35042 Rennes Cedex, France

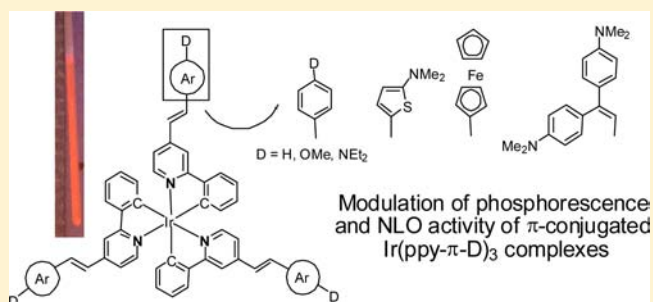
[‡]Laboratoire de Photonique Quantique et Moléculaire UMR CNRS 8531, Institut d'Alembert, ENS Cachan, 61 avenue du Président Wilson, 94235 Cachan, France

[§]Department of Chemistry, University of Durham, South Road, Durham DH1 3LE, United Kingdom

^{||}Dipartimento di Chimica dell'Università di Milano, UDR-ISTM and ISTM-CNR, Via Golgi 19, 20133 Milano, Italy

S Supporting Information

ABSTRACT: The synthesis, luminescence, and nonlinear optical properties of a new series of Ir(ppy)₃ (ppy = 2-phenylpyridine) complexes incorporating π -extended vinyl-aryl substituents at the *para* positions of their pyridine rings are reported. Appropriate substitution of the pyridyl rings allows the tuning of the luminescence properties and the second-order nonlinear optical response of this unusual family of three-dimensional chromophores. Theoretical calculations were performed to evaluate the dipole moments, to gain insight into the electronic structure, and to rationalize the observed optical properties of the investigated complexes.



INTRODUCTION

Within the field of organic materials, there is a growing interest in the study of metal complexes showing both luminescent and second-order nonlinear optical (NLO) properties as new multifunctional molecular materials which may offer additional flexibility. Their luminescent and NLO properties can be tuned by introducing charge-transfer transitions between the metal and the ligands, allowing for their fine control according to the nature, oxidation state, and coordination sphere of the metal center.¹ During the past decade, many studies of luminescent cyclometalated iridium(III) complexes have been reported.² This great interest originates from their very high-phosphorescence quantum yield and wide color tunability, which make them very attractive for applications in organic light-emitting diodes (OLEDs) for neutral complexes,³ in light-emitting electrochemical cells (LECs) for ionic complexes,⁴ and more recently in dye-sensitized solar cells.⁵ Moreover, recently we reported on various luminescent cationic cyclometalated Ir(III) complexes containing a substituted 1,10-phenanthroline^{6,7} or a 2,2'-bipyridine⁷ ligand, all of which exhibit interesting second-order NLO properties. The use of the electric field-induced second harmonic (EFISH) generation technique,⁸ supported by a sum over states time-dependent density functional theory (SOS-TDDFT) investigation, revealed that the NLO properties

are determined mainly by MLCT (metal-to-ligand charge-transfer) processes with the orbitals of the cyclometalated Ir-containing moiety acting as the donor system toward π^* -orbitals of the $N\wedge N$ bidentate ligand as the acceptor system.⁶ Also, some luminescent Ir(III) and Pt(II) complexes with a cyclometalated 2-phenylpyridine ligand in combination with a β -diketonate coligand show a significant second-order NLO response, as determined by the EFISH technique. These NLO properties can be attributed by SOS-TDDFT investigations mainly to intraligand charge-transfer transitions involving the cyclometalated ligand.⁹

These results prompted us to investigate the second-order NLO properties of neutral Ir(III) complexes bearing *three* cyclometalated 2-phenylpyridine ligands.¹⁰ We showed that an appropriate substitution of the phenyl moiety of the cyclometalated ligands may allow the tuning of the NLO response: addition of electron-withdrawing substituents on the phenyl ring of the 2-phenylpyridine ligands leads to an increase of its acceptor properties and to a NLO response dominated by MLCT transitions, whereas in the presence of a π -delocalized donor substituent, intraligand charge-transfer (ILCT) transi-

Received: March 2, 2013

Published: June 28, 2013

Scheme 1

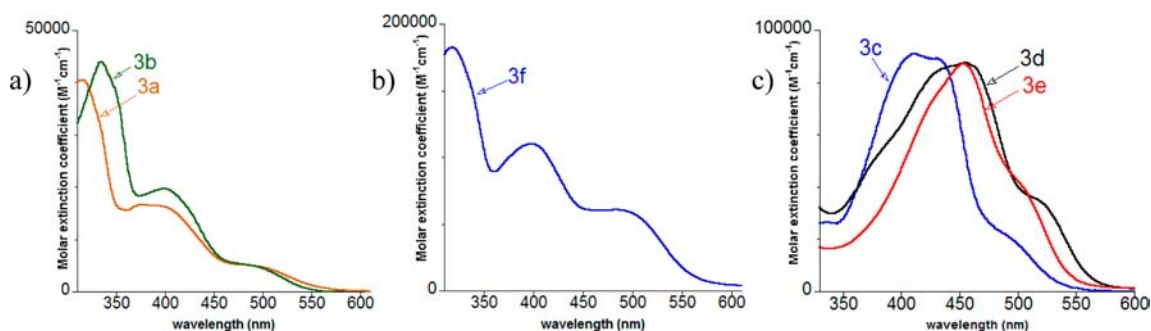
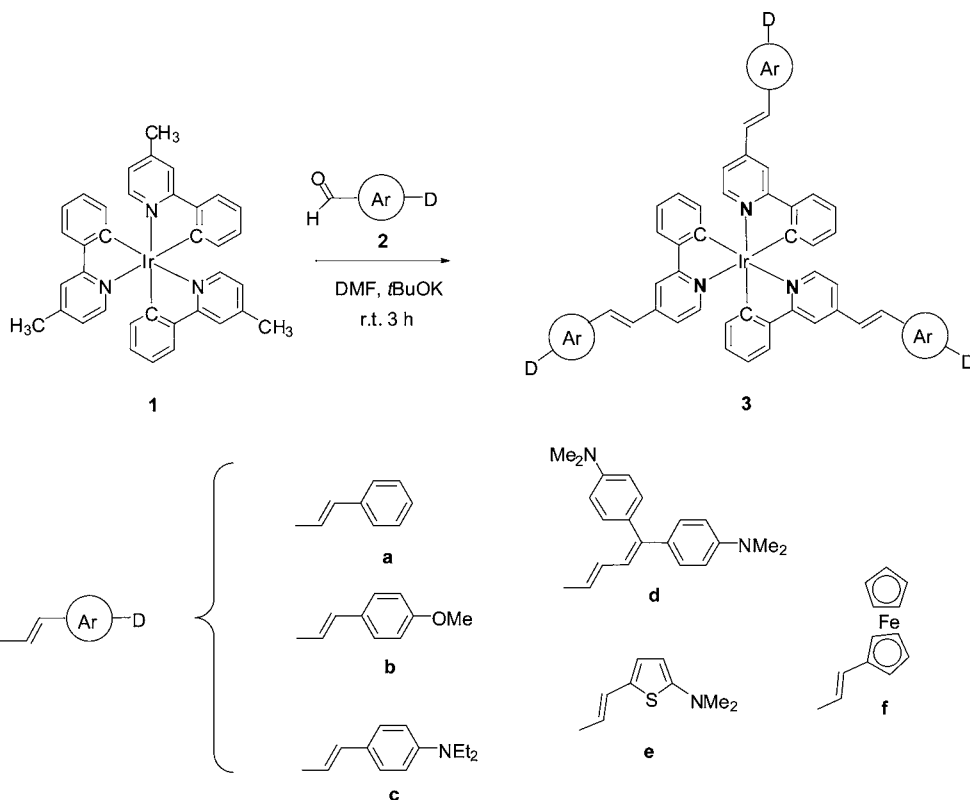


Figure 1. Absorption spectra in CH_2Cl_2 (298 K) of complexes (a) 3a and 3b, (b) 3f, and (c) 3c, 3d, and 3e.

tions control the second-order NLO properties.¹⁰ In order to get a complete portrait of this unusual family of three-dimensional (3D) chromophores, it was particularly appealing to study the effect of the nature of the substituent in the *para* position of the pyridyl moiety, which could also lead to a fine-tuning of the nonlinear optical properties by controlling the nature of charge transfers.

We describe in this Article the chemistry and the photophysical properties of a new series of iridium(III) complexes with three cyclometalated 2-phenylpyridine ligands bearing in the *para* position of the pyridyl ring a π -conjugated substituent characterized by different donor abilities. To gain a complete understanding of their second-order NLO properties, we used both the EFISH and harmonic light scattering (HLS; also called HRS for hyper-Rayleigh scattering) techniques. The linear absorption and luminescence properties are also described. To evaluate the dipole moments and to gain insight into the electronic structure and optical properties of the

investigated complexes, we performed DFT and TDDFT calculations.

RESULTS AND DISCUSSION

Design, Synthesis, and Characterization of the Complexes. The synthesis of tris-cyclometalated Ir complexes $\text{Ir}[(\text{C}\wedge\text{N})_3]$ is generally tedious and cannot be applied to chelating $\text{C}\wedge\text{N}$ ligands bearing functional groups because of the drastic reaction conditions generally required (200 °C, 48 h).¹¹ We have previously shown that, in the case of D-styryl-ppy (ppy = phenylpyridine) substituted chloro-bridged dimers $\text{Ir}[(\text{C}\wedge\text{N}-\text{ppy}-(\text{CH}=\text{CH})-(\text{C}_6\text{H}_4-\text{D})(\mu-\text{Cl})_2]$, the reaction leads to the formation of the fully hydrogenated complexes $\text{Ir}[(\text{C}\wedge\text{N}-\text{ppy}-(\text{CH}_2-\text{CH}_2)-(\text{C}_6\text{H}_4-\text{D})_3]$ (D = OMe or NEt_2).^{2c} An elegant solution to this problem is to use the so-called “chemistry-on-the-complex” approach. We found that the styryl complexes $E\text{-Ir}[(\text{C}\wedge\text{N}-\text{ppy}-(\text{CH}=\text{CH})-(\text{C}_6\text{H}_4-\text{D})_3]$ (3b, D = OMe; 3c, D = NEt_2) are accessible by direct functionalization of the metalated 4-methylphenylpyridine *fac*- $\text{Ir}[(\text{C}\wedge\text{N}-\text{ppy}-$

Me)₃ **1** using a Knoevenagel reaction. We have extended this strategy to the preparation of a family of unsaturated complexes in which unsubstituted phenyl (**3a**), (butadienyl)bis-anilino (**3d**), dimethylaminothienyl (**3e**), and ferrocenyl (**3f**) groups have been incorporated. The tris-chelate methyl complex *fac*-**1** was treated at room temperature with the requisite aldehyde **2** in the presence of *t*BuOK (Scheme 1). Under these reaction conditions, the unsaturated complexes **3a** and **3d–f** were obtained as red powders in moderate to good yields. All complexes were fully characterized by ¹H and ¹³C NMR spectroscopy and elemental analysis. They were easily identified through an AB system appearing at low field on their ¹H NMR spectra. This AB system corresponds to the vinyl protons; it shows a coupling constant of ~16 Hz, confirming the exclusive formation of the *trans* isomer. The new complexes (**3a** and **3d–f**) showed a high stability toward visible and ultraviolet light in solution. After exposure to UV irradiation for several hours (CH₂Cl₂), no change in the ¹H NMR spectra was observed, a result which contrasts with the *trans*-to-*cis* isomerization observed for **3b** and **3c** under the same conditions.^{2e}

Electronic Absorption, Photoluminescence Spectroscopy, and Computational Studies. The UV–visible spectra of the selected complexes **3a–f** in CH₂Cl₂ solution at room temperature are displayed in Figure 1. The main absorbance maxima and their extinction coefficients are compiled in Table 1. Complexes **3a** and **3b** display similar UV–visible absorption

Table 1. Absorption and Luminescence Data for Ir Complexes **1** and **3a–f**

	λ_{abs} (nm) (ϵ (M ⁻¹ cm ⁻¹)) ^a	λ_{em} (nm) ^b	τ (μ s)
1	282 (39000), 342 (8700), 378 (9400), 407 (6100), 447 (2700), 478 (1100)	495	1.4
3a ^{2e}	315 (40464), 402 (16137), 499 (4711)	615, ^c 673, 740	2.3
3b	334 (43878), 402 (19618), 499 (4565)	613, ^c 677, 741	4.3
3c ^{2e}	412 (91000), 432 (90000), 497 (19000)	650, ^c 673, 740	10.2
3d	377 (33180), 454 (87533), 525 (21047)	– ^d	–
3e	416 (sh), 455 (87155), 503 (42672)	703, ^c 784	16
3f	318 (185957), 398 (118811), 493 (67147)	– ^d	–

^aAt 298 K in CH₂Cl₂. ^bAt 77 K in ether/isopentane/ethanol (2:2:1, v/v). ^c λ_{max} . ^dNo emission was detectable for these complexes.

patterns, with intense absorption bands at ~310–350 nm and two moderately intense lower-energy bands around 360–460 and 460–560 nm (Figure 1a). With reference to previous studies on iridium(III) complexes,^{2e} the high-energy absorption bands are assigned to intraligand π – π^* transitions of the styrylphenylpyridine ligands, while the low-energy absorption bands are assigned to MLCT transitions. The band tailing further into the visible (up to 560 nm) may be due to excitation to the triplet CT states, as typically observed in related bis-cyclometalated iridium(III) complexes.¹² The ferrocenyl derivative **3f** displays similar MLCT absorption energies (Figure 1b).

The presence of the strong electron-donating amino substituent in **3c**, **3d**, and **3e** gives rise to an additional broad absorption band at lower energy assigned to an ILCT transition, the pyridine ligand acting as a π^* -acceptor group. The replacement of the phenyl ring in **3c** by a thienyl group in **3e** induces a significant red-shift ($\Delta = 43$ nm, 2294 cm⁻¹) of

this band, probably reflecting destabilization of the highest occupied molecular orbital (HOMO) by the more delocalized thiophene ring. Absorption bands due to MLCT transitions are typically anticipated around 400 nm for [Ir(CAN-ppy)₃] complexes^{11,13} and are obscured in these cases.

DFT and TDDFT computations (see Computational Studies; full results are given in the Supporting Information) fully confirm the given assignment. For instance, it can be seen that the TDDFT-simulated UV–vis absorption spectra of **3c** and **3d** (Figure 2) resemble nicely the experimental ones, thus

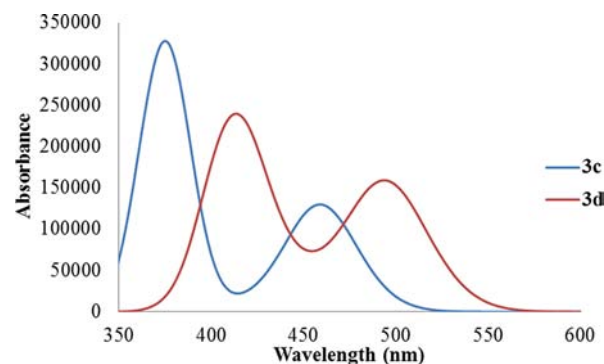


Figure 2. TDDFT-simulated absorption spectra of **3c** and **3d**.

permitting us to assign the observed bands with confidence. It must be noted that the TDDFT computations were carried out considering isolated molecules, whereas the absorption spectra have been recorded in CH₂Cl₂ solution; this is partly responsible for the systematic blue shift of the theoretical bands relative to the experimental ones.

For **3c**, the lowest-energy absorption band at 463 nm ($\lambda_{\text{exp}} = 497$ nm) involving HOMO-1 and HOMO-2 to LUMO transitions is mainly a MLCT excitation whereas the band at 379 nm ($\lambda_{\text{exp}} = 412$ nm), which corresponds to HOMO-3, HOMO-4, and HOMO-5 to LUMO and to a smaller extent to LUMO+1 and LUMO+2 transitions, is attributed to an ILCT excitation (intraligand π – π^* transitions). These assignments are based on the frontier molecular orbital (MO) diagrams shown in Figure 3. The metal contribution in the occupied MOs of **3c** is 45%, 34%, and 36% for HOMO, HOMO-1, and HOMO-2, respectively, whereas the percentage decreases from HOMO-3 to HOMO-8. As expected, cyclic voltammetry confirms the trend of the HOMOs obtained by DFT calculations (see Supporting Information).

Upon photoexcitation at 450 nm, all of the styryl complexes **3a–f** are non-emissive in fluid solution (CH₂Cl₂) at room temperature. At 77 K in EPA (ether/isopentane/ethanol 2:2:1, v/v), they display a structured emission profile centered at ca. 615 nm (**3a** and **3b**), 650 nm (**3c**), and 703 nm (**3e**). Data are compiled in Table 1, and representative spectra are shown in Figure 4. Red phosphorescence can be observed from Ir(III) complexes **3a–c** and **3e** bearing substituted cyclometalated phenyl (ppy) ligands to raise the emission energy relative to that of the efficient green phosphor starting complex *fac*-Ir(ppy-Me)₃ **1**. The incorporation of the π -conjugated vinyl system induces a red-shifted emission, and the emission wavelength of the styryl complexes increases in the order H, OMe < NEt₂ < thio-NMe₂. The energy level of excited states of Ir complexes is strongly affected by the nature of the π -conjugated group. We assume that the luminescence from the cyclometalated Ir(III) complexes **3a** and **3b** originates from the admixture of ligand-

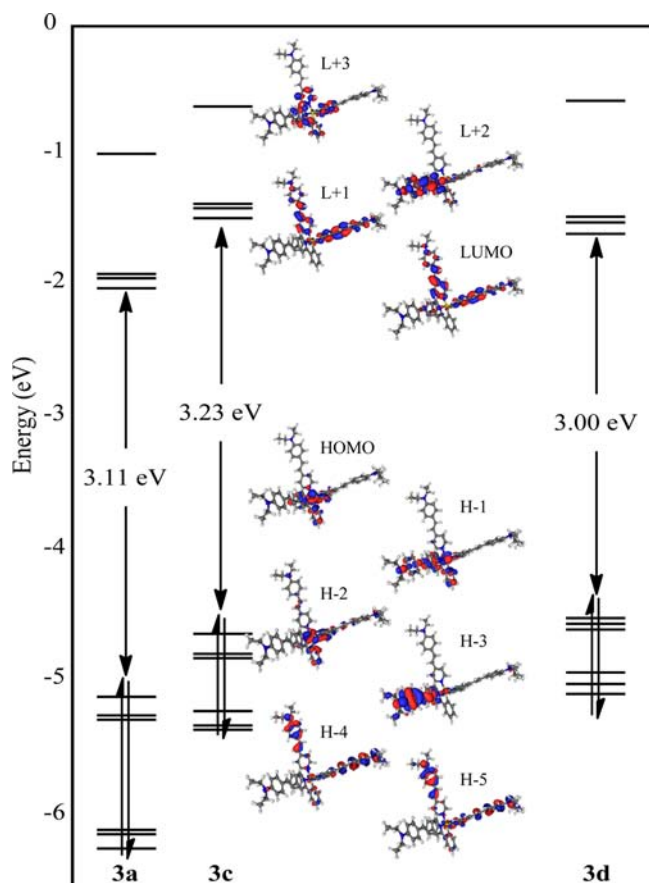


Figure 3. Energy level diagram of 3a, 3c, and 3d and frontier MOs of 3c.

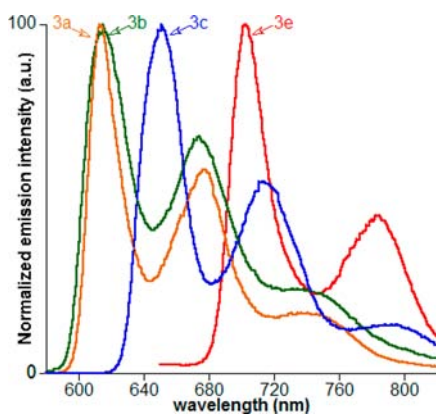


Figure 4. Emission spectra of 3a–c and 3e (77 K, EPA). $\lambda_{exc} = 450$ nm.

centered IL $^3(\pi-\pi^*)$ states and MLCT states through spin-orbit coupling,^{2e} while the amino derivatives 3c and 3e emit mainly from an $^3\text{ILCT}$ excited state. Complexes 3d and 3f are non-emissive at low temperature, and we could not detect any emission band, even by using a CCD-camera operating in the near IR. It is possible that in these complexes a photoinduced electron-transfer mechanism of quenching, involving the readily oxidizable substituents as electron donors, is involved. Indeed, ferrocene is well-known to act as a quencher of many luminescent systems, via either electron-transfer or energy-transfer processes.¹⁴ In the field of inorganic photochemistry, a number of examples have been reported with the archetypal

emitter $[\text{Ru}(\text{bpy})_3]^{2+}$ and its derivatives, involving both intra- and intermolecular quenching.^{15a,b} Studies have also revealed very efficient intramolecular quenching of the triplet state of platinum diimine bisacetylide complexes by π -conjugated ferrocene units $[\text{Pt}(\text{N}\wedge\text{N})(-\text{C}\equiv\text{C}-\text{Fc})_2]$, which incorporate linkers not dissimilar to the linkers used in our study.^{15c}

Quadratic NLO Studies. In order to investigate their second-order NLO properties, the selected Ir(III) complexes 3a–f were first investigated by the EFISH technique. It is known that the EFISH technique⁸ can provide direct information on the intrinsic molecular NLO properties through eq 1:

$$\gamma_{\text{EFISH}} = (\mu\beta_{\text{EFISH}}/5kT) + \gamma(-2\omega; \omega, \omega, 0) \quad (1)$$

where $\mu\beta_{\text{EFISH}}/5kT$ is the dipolar orientational contribution to the molecular nonlinearity, and $\gamma(-2\omega; \omega, \omega, 0)$, the third-order polarizability at frequency ω of the incident light, is a purely electronic cubic contribution to γ_{EFISH} which can usually be neglected when studying the second-order NLO properties of dipolar compounds because the cubic γ_{THG} values are less than 10% of the γ_{EFISH} values.¹⁶

In Table 2 are reported the $\mu\beta_{\text{EFISH}}$ values of all the investigated complexes, along with that previously reported for

Table 2. $\mu\beta_{\text{EFISH}}$, μ , β_{EFISH} , and $\langle\beta_{\text{HLS}}\rangle$ of the Investigated Ir(III) Complexes

	$\mu\beta_{\text{EFISH}}^a \times 10^{-48}$ esu	$\mu^b \times 10^{-18}$ esu	$\beta_{\text{EFISH}} \times 10^{-30}$ esu	$\langle\beta_{\text{HLS}}\rangle^b \times 10^{-30}$ esu
1 ¹⁰	1050	7.5	140	– ^c
3a	–640	8.0	–80	250
3b	–700	12.8	–54	290
3c	480	14.5	33	400
3d	620	17.1	36	460
3e	830	14.3	58	330
3f	–430	8.5	–51	330

^aValues obtained working at a concentration of 10^{-3} M; estimated uncertainty in EFISH and HLS measurements is $\pm 10\%$ and $\pm 15\%$, respectively. ^bCalculated dipole moment. ^cCould not be measured because of sparking of the sample.

1,¹⁰ measured in a CH_2Cl_2 solution (concentration = 10^{-3} M) with an incident wavelength of 1.907 μm . To obtain β_{EFISH} , the projection along the dipole moment axis of the vectorial component of the tensor of the quadratic hyperpolarizability, it is necessary to know the dipole moment, μ . In the present study, we used the DFT-computed dipole moments (see Computational Studies) for complexes 3a–e calculated in a vacuum from their optimized geometries shown in Figure 5 (optimized geometries in the Supporting Information). All complexes exhibit the expected octahedral geometry with the three ligands arranged in a *facial* fashion, which is in agreement with the experimental crystal structure of *fac*-Ir(ppy)₃.¹⁷ The DFT-computed Ir–C and Ir–N bond lengths, ca. 2.003 and 2.130 Å, respectively, in all complexes 3a–f, compare very well with the X-ray values for *fac*-Ir(ppy)₃¹⁷ equal to 2.03 and 2.09 Å. The computed Ir–C and Ir–N bond lengths are in agreement with previous DFT calculations.²¹ Moreover, it must be pointed out that for all complexes the styryl groups are coplanar with the adjacent pyridine ring.

As evidenced in Table 2, the selected complexes 3a–f are characterized by a high absolute value of $\mu\beta_{\text{EFISH}}$ ($430\text{--}830 \times 10^{-48}$ esu). It appears that substitution of the methyl group in

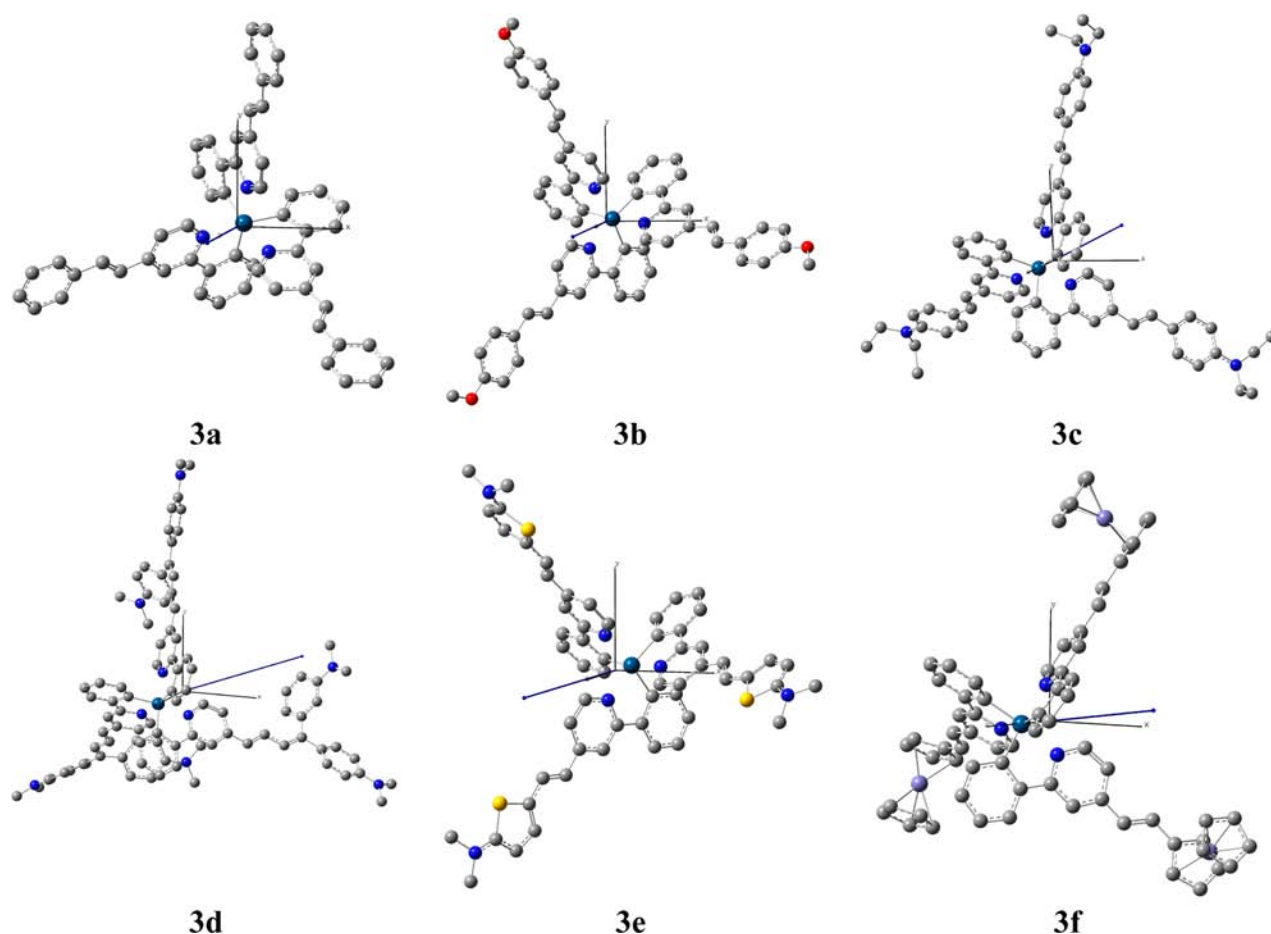


Figure 5. Optimized geometries of complexes 3a–f. The Ir–N bond is not shown, and H atoms are omitted for clarity (ground-state dipole moment is represented by the blue arrow).

the *para* position of the pyridine ring (complex **1**) by a π -delocalized styryl moiety (complex **3a**) does not affect significantly the ground-state dipole moment but leads to an inversion of the sign of β_{EFISH} . The negative value observed for **3a** (-80×10^{-30} esu) reflects the negative value of $\Delta\mu_{\text{eg}}$ (difference between the excited dipole moment and the ground-state dipole moment, values given in the Supporting Information).¹ Indeed, according to the two-level model, β_{EFISH} is proportional to $\Delta\mu_{\text{eg}}$. The decrease of the dipole moment upon excitation is in agreement with a second-order NLO response dominated by MLCT transitions where the charge transfer from the iridium center to the phenylpyridine ligands is in opposition to the direction of the components of the dipole moment.¹⁸ The introduction of a weak donor methoxy substituent in the *para* position of the styryl group (**3b**) also leads to a negative β_{EFISH} but with a lower absolute value (-54×10^{-30} esu), in agreement with ILCT transitions vectorially opposed to the MLCT transitions that also contribute to the NLO response. When the methoxy group is replaced by a stronger donor moiety such as diethylamino (**3c**), the importance of ILCT transitions prevails on the MLCT ones and the β_{EFISH} becomes positive (33×10^{-30} esu). In the case of complex **3e**, which has a NMe₂-thienyl moiety instead of a NEt₂-phenyl group, the positive quadratic hyperpolarizability is even higher (58×10^{-30} esu), as expected from the significant red-shift of the ILCT on going from **3c** to **3e** (Figure 1). Our data provide evidence that the donor strength of the ferrocene moiety is similar to that of the methoxyphenyl group in these

cyclometalated Ir(III) complexes (e.g., **3b** vs **3f**), as previously observed for other NLO systems.²

As all the investigated tris-cyclometalated Ir(III) complexes are 3D chromophores with C₃ symmetry, they can be viewed as multipolar molecules having both dipolar ($\beta^{(1)}$) and octupolar ($\beta^{(3)}$) contributions. Because the EFISH technique gives only the dipolar contribution to the second-order NLO response, it was of particular importance to study the various complexes also by the HLS technique, which reflects both the dipolar and octupolar components.¹⁹ As shown in Table 2, all the investigated Ir(III) complexes are characterized by a large value of $\langle\beta_{\text{HLS},1.907}\rangle$ ($250\text{--}460 \times 10^{-30}$ esu). Comparison of the trio **3a–c** having the same backbone with different end groups on the styryl fragment (H, OMe, NEt₂) allows the systematic study of the effect of end groups on the NLO response of these complexes. An increase of the electron-donating strength of the end group leads to an increase of the β_{HLS} values following the trend of **3a** < **3b** < **3c**. This is in agreement with the absorption spectra of these complexes that show a progressive red shift upon going from H to OMe to NEt₂, the latter showing a strong ILCT band that is responsible for the large increase of the β_{HLS} value compared to those of H (**3a**) and OMe (**3b**). In addition to the nature of the end group, the π -conjugated system itself was found to have a further influence on the NLO properties. Complexes **3c**, incorporating an amino-*phenyl* substituent, and **3e**, incorporating an amino-*thienyl* substituent, present β_{HLS} values similar to those reported for ruthenium and zinc tris-bipyridine complexes incorporating styryl amino

substituents²⁰ and to that found for cationic cyclometalated Ir(III) complexes containing two cyclometalated 2-phenylpyridine ligands and a substituted 1,10-phenanthroline or 2,2'-bipyridine ligand where the major contribution to the total quadratic hyperpolarizability is controlled by the octupolar part. Remarkably, complex **3d**, having a (butadienyl)bis-anilino substituent, showed the highest NLO activity ($\beta_{\text{HLS}} = 460 \times 10^{-30}$ esu). This behavior is not surprising because two conjugated and highly electron-withdrawing substituents are used as end groups in **3d**. Finally, it is worth noting that all the investigated chromophores display much larger β_{HLS} versus β_{EFISH} values, suggesting a much higher octupolar contribution to the total quadratic hyperpolarizability of this family of tris-cyclometalated phenylpyridine iridium complexes, as previously observed in the case of subphthalocyanine chromophores with C_3 symmetry.²¹

CONCLUSION

We have synthesized and measured the luminescence and NLO properties of a new series of neutral iridium(III) complexes Ir(ppy)₃ incorporating π -extended vinyl-aryl substituents at their pyridyl *para* positions. Some of these complexes display red phosphorescence at 77 K originating from a mixed ³MLCT and ³ILCT excited state for complexes bearing strong electron-donating amino substituents (**3c** and **3e**) and from mixed ³MLCT and ³IL excited states for complexes bearing weaker electron-donating substituents (**3a** and **3b**). These multipolar complexes present strong NLO activity measured by HLS and EFISH techniques. EFISH measurements of the investigated complexes showed that they display a high absolute $\mu\beta_{\text{EFISH}}$ value with a positive sign when the NLO response is dominated by ILCT transitions (**3c–e**) and a negative sign when the response is dominated by MLCT transitions (**3a**, **3b**, and **3f**). HLS results indicated that a higher β value is obtained for complexes incorporating stronger electron-donating end groups, with complex **3d** incorporating the (butadienyl)bis-anilino substituent showing the highest value. Finally, a comparison between the EFISH and HLS data suggests that the major contribution to the quadratic hyperpolarizability is controlled mainly by the octupolar portion. DFT and TDDFT computations provided a rationalization of the observed optical properties. In conclusion, the investigated complexes are luminescent and highly active second-order NLO chromophores with a response easily tunable by a rational approach. Their known high stability makes them particularly appealing for NLO applications.

EXPERIMENTAL SECTION

General Procedure. All manipulations were performed using Schlenk techniques under an Ar atmosphere. All solvents were dried and purified by standard procedures. NMR spectra were recorded on Bruker AV 400 or AV 500 MHz spectrometers. ¹H and ¹³C chemical shifts are given versus SiMe₄ and were determined by reference to residual ¹H and ¹³C solvent signals. Attribution of carbon atoms was based on HMBC, HMQC, and COSY experiments. Elemental analyses were performed at the Centre de Mesures Physiques de l'Ouest in Rennes. Complex **1** was prepared according to a literature procedure.¹¹ The thienyl derivative **2e** was prepared following a reported procedure.²² The aldehyde 3,3-bis(4-(dimethylamino)phenyl)acrylaldehyde was provided by C. Mayer.²³

UV–Visible Absorption and Emission Studies. UV–visible absorption spectra were recorded using a UVIKON 9413 or Biotek Instruments XS spectrophotometer using quartz cuvettes of 1 cm path length. Steady-state luminescence spectra were measured using a Jobin

Yvon FluoroMax-2 or Tau-3 spectrofluorimeter, fitted with a red-sensitive Hamamatsu R928 photomultiplier tube. The spectra shown are corrected for the wavelength dependence of the detector, and the quoted emission maxima refer to the values after correction. Lifetimes were measured by time-correlated single-photon counting (TCSPC) following excitation at 374 nm with a pulsed laser diode, and the emitted light was detected at right angles using an R928 photomultiplier tube after passage through a monochromator. The lifetime of **3e** was too long to measure using this method and was instead obtained by multichannel scaling following excitation with a microsecond-pulsed xenon lamp.

EFISH Measurements. All EFISH⁸ measurements were carried out at the Dipartimento di Chimica of the Università degli Studi di Milano. Measurements were performed using CH₂Cl₂ solutions at a concentration of 1×10^{-3} M and with a nonresonant incident wavelength of 1.907 μm , obtained by Raman-shifting the fundamental 1.064 μm wavelength produced by a Q-switched, mode-locked Nd³⁺:YAG laser manufactured by Atalaser. The apparatus for the EFISH measurements was a prototype made by SOPRA (Bois-Colombes, France). The $\mu\beta_{\text{EFISH}}$ values reported are the mean values of 16 successive measurements performed on the same sample.

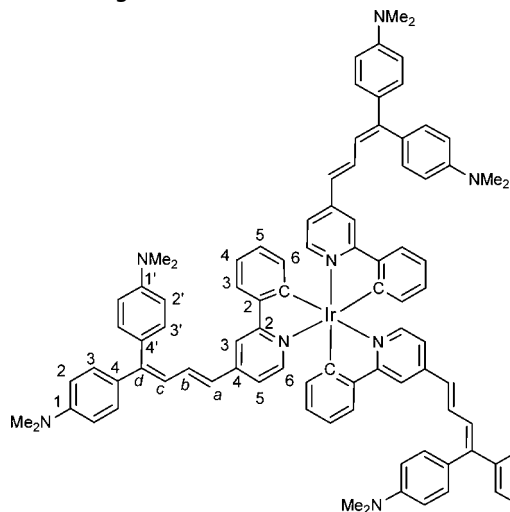
HLS Measurements. The HLS technique¹⁹ involves the detection of the incoherently scattered second harmonic generated by a solution of the molecule under irradiation with a laser of wavelength λ leading to the measurement of the mean value of the $\beta \times \beta$ tensor product, $\langle\beta_{\text{HLS}}\rangle$. All HLS measurements were carried out at the Ecole Normale Supérieure de Cachan. Measurements were performed using CH₂Cl₂ solutions at a concentration of 1×10^{-3} M and a low-energy nonresonant incident radiation of 1.907 μm .

Synthesis of fac-Ir(CAN-ppy-CH=CH-Ar-D)₃. In a Schlenk tube, to a solution of fac-Ir(CAN-ppy-4-Me)₃ (**1**) (160 mg, 0.23 mmol) in 20 mL of DMF were added the appropriate aldehyde (0.92 mmol) and tBuOK (103 mg, 0.92 mmol). The reaction mixture was stirred at room temperature for 3 h. Addition of 20 mL of water allowed an orange-red powder to precipitate. The precipitate was filtered off and washed with MeOH and Et₂O. The solid was dried in vacuum.

Ir[CAN-ppy-CH=CH-C₆H₅]₃ (3a**).** Red powder, 58% yield. ¹H NMR (400 MHz, CD₂Cl₂) δ : 8.05 (s, 1H, Py³), 7.81 (d, ³J = 7.6 Hz, 1H, Ph³), 7.65 (d, ³J = 5.8 Hz, 1H, Py⁶), 7.62 (m, 2H, C₆H₅), 7.42 (m, 4H, C₆H₅, =CH), 7.17 (d, ³J = 16 Hz, 1H, =CH), 7.11 (d, ³J = 5.8 Hz, 1H, Py⁵), 6.96 (t, ³J = 6.9 Hz, 1H, Ph⁴), 6.85 (m, 2H, Ph⁵, Ph⁶). ¹³C [¹H] NMR (100 MHz, CD₂Cl₂) δ : 166.6 (C²-Py), 161.3 (C¹-Ph), 147.1 (C⁶-Py), 144.9 (C⁴-Py), 143.8 (C²-Ph), 136.9 (C⁶-Ph), 136.1 (C¹-C₆H₄), 133.8 (=CH), 129.6 (C⁵-Ph), 128.9 (C₆H₅), 128.8 (C₆H₅), 127.1 (C₆H₅), 125.6 (=CH), 123.9 (C³-Ph), 119.9 (C⁴-Ph), 119.2 (C⁵-Py), 116.1 (C³-Py). Anal. Calcd for [C₅₇H₄₂N₃Ir-CH₂Cl₂]: C, 66.59; H, 4.24; N, 4.02. Found C, 66.45; H, 4.18; N, 4.23.

Ir[CAN-ppy-CH=CH-CH=C(C₆H₄-NMe₂)₂]₃ (3d**).** Red powder, 58% yield. ¹H NMR (500 MHz, CD₂Cl₂) δ : 7.74 (s, 1H, Py³), 7.66 (d, ³J = 7.6 Hz, 1H, Ph³), 7.41 (d, ³J = 6 Hz, 1H, Py⁶), 7.25 (m, 3H, C₆H₄, =CH), 7.14 (d, ³J = 8.2 Hz, 2H, C₆H₄), 6.89 (t, 1H, Ph⁴), 6.75 (m, 8H, Py⁵, Ph⁵, Ph⁶, C₆H₄, C₆H₄, =CH), 6.62 (d, ³J = 15.5 Hz, 1H, =CH), 3.03 (s, 6H, NCH₃), 3.01 (s, 6H, NCH₃). ¹³C [¹H] NMR (125 MHz, CD₂Cl₂) δ : 166.1 (C²-Py), 161.5 (C¹-Ph), 150.5 (C¹-C₆H₄), 150.3 (C¹-C₆H₄), 147.9 (=CH), 146.6 (C⁶-Py), 145.8 (C⁴-Py), 143.9 (C²-Ph), 136.8 (C⁶-Ph), 133.9 (=CH), 131.7 (C₆H₄), 130.2 (C₆H₄), 129.3 (C⁵-Ph), 129.1 (C₆H₄), 127.2 (C₆H₄), 126.7 (=CH), 123.7 (C³-Ph), 122.6 (=CH), 119.6 (C⁴-Ph), 118.3 (C⁵-Py), 115.6 (C³-Py), 111.7 (C₆H₄), 111.6 (C₆H₄), 40.2 (NCH₃), 40.1 (NCH₃). Anal. Calcd for C₉₃H₉₀N₉Ir-CH₂Cl₂: C, 70.08; H, 5.76; N, 7.83. Found: C, 70.39; H, 5.84; N, 7.56.

Numbering.



$\text{Ir}[\text{C}^{\wedge}\text{N-ppy-CH}=\text{CH}-(2,5\text{-C}_4\text{H}_2\text{S}(\text{NMe}_2))]_3$ (**3e**). Red powder, 36% yield. ^1H NMR (400 MHz, CD_2Cl_2) δ : 7.86 (s, 1H, Ph^3), 7.74 (d, $^3J = 7.7$ Hz, 1H, Ph^3), 7.51 (d, $^3J = 6$ Hz, 1H, Py^6), 7.38 (d, $^3J = 16$ Hz, 1H, $=\text{CH}$), 6.92 (m, 3H, Py^5 , Ph^4 , thio), 6.85–6.80 (m, 2H, Ph^5 , Ph^6), 6.46 (d, $^3J = 16$ Hz, 1H, $=\text{CH}$), 5.82 (d, $^3J = 4$ Hz, 1H, thio), 3.03 (s, 6H, CH_3). ^{13}C [^1H] NMR (100 MHz, CD_2Cl_2) δ : 166.1 ($\text{C}^2\text{-Py}$), 161.5 ($\text{C}^1\text{-Ph}$), 160.5 ($\text{C}^4\text{-thio}$), 146.8 ($\text{C}^6\text{-Py}$), 145.6 ($\text{C}^4\text{-Py}$), 144.1 ($\text{C}^2\text{-Ph}$), 136.8 ($\text{C}^6\text{-Ph}$), 131.1 (thio), 129.3 ($\text{C}^5\text{-Ph}$), 127.9 ($=\text{CH}$), 125.6 (thio), 123.6 ($\text{C}^3\text{-Ph}$), 119.6 ($\text{C}^4\text{-Ph}$), 118.1 ($\text{C}^5\text{-Py}$), 118.0 ($=\text{CH}$), 114.8 ($\text{C}^3\text{-Py}$), 101.8 (thio), 42.1 (CH_3). Anal. Calcd for $\text{C}_{57}\text{H}_{51}\text{IrN}_6\text{S}_3\cdot\text{CH}_2\text{Cl}_2$: C, 58.37; H, 4.48; N, 7.04. Found: C, 58.46; H, 4.43; N, 7.04.

$\text{Ir}[\text{C}^{\wedge}\text{N-ppy}(\text{CH}=\text{CH})(\eta^5\text{-C}_5\text{H}_5)\text{Fe}(\eta^5\text{-C}_5\text{H}_5)]_3$ (**3f**). Red powder, 33% yield. ^1H NMR (400 MHz, CD_2Cl_2) δ : 7.95 (s, 1H, Py^3), 7.79 (d, $^3J = 7.3$ Hz, 1H, Ph^3), 7.62 (d, $^3J = 6$ Hz, 1H, Py^6), 7.24 (d, $^3J = 16$ Hz, 1H, $=\text{CH}$), 7.02 (d, $^3J = 6$ Hz, 1H, Py^5), 6.96 (t, $^3J = 7.8$ Hz, 1H, Ph^4), 6.87–6.80 (m, 2H, Ph^5 , Ph^6), 6.73 (d, $^3J = 16$ Hz, 1H, $=\text{CH}$), 4.59–4.57 (m, 2H, C_5H_4), 4.42 (m, 2H, C_5H_4), 4.19 (s, 5H, C_5H_5). ^{13}C [^1H] NMR (100 MHz, CD_2Cl_2) δ : 166.1 ($\text{C}^2\text{-Py}$), 161.5 ($\text{C}^1\text{-Ph}$), 147.0 ($\text{C}^6\text{-Py}$), 145.3 ($\text{C}^4\text{-Py}$), 144.0 ($\text{C}^2\text{-Ph}$), 136.8 ($\text{C}^6\text{-Ph}$), 133.5 ($=\text{CH}$), 129.5 ($\text{C}^5\text{-Ph}$), 123.8 ($\text{C}^3\text{-Ph}$), 122.5 ($=\text{CH}$), 119.7 ($\text{C}^4\text{-Ph}$), 118.5 ($\text{C}^5\text{-Py}$), 115.2 ($\text{C}^3\text{-Py}$), 81.5 (C_5H_4), 70.0 (C_5H_4), 69.4 (C_5H_5), 67.6 (C_5H_4). Anal. Calcd for $\text{C}_{69}\text{H}_{54}\text{Fe}_3\text{IrN}_3\cdot 0.33\text{CH}_2\text{Cl}_2$: C, 63.41; H, 4.20; N, 3.20. Found: C, 63.53; H, 4.37; N, 3.37.

Computational Studies. DFT computations have been performed in order to determine the geometrical and electronic structures of the complexes under consideration. The PBE0 hybrid functional²⁴ has been chosen with the LanL2DZ basis set²⁵ augmented with polarization functions on all atoms, except hydrogen. The optimizations of the geometries were carried out first; the optimized geometries of all species were characterized as true minima on the potential energy surfaces using vibration frequency calculations. Then, in order to compute their electronic spectra, TDDFT calculations were performed considering their optimized geometries. The program used for the DFT and TDDFT computations was Gaussian 09.²⁶ Representations of molecular structures and orbitals were made using the Molekel program.²⁷

ASSOCIATED CONTENT

Supporting Information

Computed dipole moments, weights of Ir 5d orbitals in the HOMOs, TD-DFT results, Ir–C and Ir–N computed bond lengths, and DFT-optimized structures. This material is available free of charge via the Internet at <http://pubs.acs.org>.

AUTHOR INFORMATION

Corresponding Author

*E-mail: veronique.guerchais@univ-rennes1.fr (V.G.), dominique.roberto@unimi.it (D.R.). Phone: +33223236729 (V.G.), +390250314399 (D.R.). Fax: +3223236939 (V.G.), +390250314405 (D.R.).

Notes

The authors declare no competing financial interest.

ACKNOWLEDGMENTS

We deeply thank Dr. Stefania Righetto and Dr. Mirko Magni for experimental help and fruitful discussions. This work was supported by the ANR-COMET program, LEA MMC Rennes-Durham, Fondazione Cariplo (Grant 2010-0525), and MIUR (FIRB 2003: RBNE033KMA and FIRB 2004: RBPRO5JH2P). Special thanks to Dr. C. Mayer for providing the 3,3-bis(4-(dimethylamino)phenyl)acrylaldehyde. The authors are grateful to GENCI-IDRIS and GENCI-CINES for an allocation of computing time (Grant 2011-080649).

DEDICATION

Dedicated to Professor Renato Ugo on the occasion of his 75th birthday.

REFERENCES

- (1) For NLO properties, see for example: (a) Coe, B. J. In *Comprehensive Coordination Chemistry II*; Elsevier Pergamon: Oxford, U.K., 2004; Vol. 9, pp 621–687. (b) Maury, O.; Le Bozec, H. *Acc. Chem. Res.* **2005**, *38*, 691–704. (c) Cariati, E.; Pizzotti, M.; Roberto, D.; Tessore, F.; Ugo, R. *Coord. Chem. Rev.* **2006**, *250*, 1210–1233. (d) Coe, B. J. *Acc. Chem. Res.* **2006**, *39*, 383–393. (e) Morrall, J. P.; Dalton, G. T.; Humphrey, M. G.; Samoc, M. *Adv. Organomet. Chem.* **2007**, *55*, 61–136. (f) Di Bella, S.; Dragonetti, C.; Pizzotti, M.; Roberto, D.; Tessore, F.; Ugo, R. In *Topics in Organometallic Chemistry* 28; Le Bozec, H., Guerchais, V., Eds.; Springer-Verlag: Berlin, Germany, 2010; Vol. 28, pp 1–55. (g) Maury, O.; Le Bozec, H. *Molecular Materials*; Bruce, D. W., O'Hare, D., Walton, R. I., Eds.; Wiley: Chichester, U.K., 2010; pp 1–59. For luminescence properties, see for example: (h) Evans, R. C.; Douglas, P.; Winscom, C. J. *Coord. Chem. Rev.* **2006**, *250*, 2093–2126. (i) You, Y.; Nam, W. *Chem. Soc. Rev.* **2012**, *41*, 7061–7084. (j) Chi, Y.; Chou, P. T. *Chem. Soc. Rev.* **2010**, *39*, 638–655. (k) Wong, W.-Y.; Ho, C.-L. *J. Mater. Chem.* **2009**, *19*, 4457–4482. (l) Zhao, Q.; Li, F.; Huang, C. *Chem. Soc. Rev.* **2010**, *39*, 3007–3030. (m) Yersin, H.; Rausch, A.; Czerwieniec, R.; Hofbeck, T.; Fischer, T. *Coord. Chem. Rev.* **2011**, *255*, 2622–2652.
- (2) (a) Baldo, M. A.; Lamansky, S.; Burrows, P. E.; Thompson, M. E.; Forrest, S. R. *Appl. Phys. Lett.* **1999**, *75*, 4–6. (b) Crabtree, R. H.; Mingos, D. M. *Comprehensive Organometallic Chemistry III*; Elsevier: Oxford, U.K., 2007; Vol. 12. (c) Wong, W.-Y.; Ho, C.-L. *Coord. Chem. Rev.* **2009**, *253*, 1709–1758. (d) Liu, Z.; Bian, Z.; Huang, C. *Top. Organomet. Chem.* **2010**, *28*, 113–142. (e) Lepeltier, M.; Le Bozec, H.; Guerchais, V.; Lee, T. K. M.; Lo, K. K. W. *Organometallics* **2005**, *24*, 6069–6072. (f) Wilkinson, A. J.; Goeta, A. E.; Foster, C. E.; Williams, J. A. G. *Inorg. Chem.* **2004**, *43*, 6513–6515. (g) Dragonetti, C.; Falciola, L.; Mussini, P.; Righetto, S.; Roberto, D.; Ugo, R.; Valore, A.; De Angelis, F.; Fantacci, S.; Sgamellotti, A.; Ramon, M.; Muccini, M. *Inorg. Chem.* **2007**, *46*, 8533–8547. (h) De Angelis, F.; Fantacci, S.; Evans, N.; Klein, C.; Zakeeruddin, S. M.; Moser, J. E.; Kalyanasundaram, K.; Bolink, H. J.; Graetzel, M.; Nazeeruddin, M. K. *Inorg. Chem.* **2007**, *46*, 5989–6001. (i) Hay, P. J. *J. Phys. Chem. A* **2002**, *106*, 1634–1641. (j) Zhou, G.; Wong, W.-Y.; Yang, X. *Chem.—Asian J.* **2011**, *6*, 1706–1727. (k) Zhou, G.; Wong, W.-Y.; Suo, S. *J. Photochem. Photobiol., C* **2010**, *11*, 133–156.
- (3) See for example: (a) Nazeeruddin, M. K.; Humphrey-Baker, R.; Berner, D.; Rivier, S.; Zuppiroli, L.; Graetzel, M. *J. Am. Chem. Soc.* **2003**, *125*, 8790–8797. (b) Tsuboyama, A.; Iwawaki, H.; Furugori, M.;

- Mukaide, T.; Kamatani, J.; Igawa, S.; Moriyama, T.; Miura, S.; Takiguchi, T.; Okada, S.; Hoshino, M.; Ueno, K. *J. Am. Chem. Soc.* **2003**, *125*, 12971–12979. (c) Hwang, F. M.; Chen, H. Y.; Chen, P. S.; Liu, C. S.; Chi, Y.; Shu, C. F.; Wu, F. L.; Chou, P. T.; Peng, S. M.; Lee, G. H. *Inorg. Chem.* **2005**, *44*, 1344–1353. (d) Okada, S.; Okinaka, K.; Iwakaki, H.; Furugori, M.; Hashimoto, M.; Mukaide, T.; Kamatani, J.; Igawa, S.; Tsuboyama, A.; Takiguchi, T.; Ueno, K. *Dalton Trans.* **2005**, *9*, 1583–1590. (e) Zhou, G.; Ho, C.-L.; Wong, W.-Y.; Wang, Q.; Ma, D.; Wang, L.; Lin, Z.; Marder, T. B.; Beeby, A. *Adv. Funct. Mater.* **2008**, *18*, 499–511. (f) Ho, C.-L.; Wang, Q.; Lam, C.-S.; Wong, W.-Y.; Ma, D.; Wang, L.; Gao, Z.-Q.; Chen, C.-H.; Cheah, K.-W.; Lin, Z. *Chem.—Asian J.* **2009**, *4*, 89–103. (g) Ho, C.-L.; Chi, L.-C.; Hung, W.-Y.; Chen, W.-J.; Lin, Y.-C.; Wu, H.; Mondal, E.; Zhou, G.-J.; Wong, K.-T.; Wong, W.-Y. *J. Mater. Chem.* **2012**, *22*, 215–224.
- (4) (a) Lowry, M. S.; Goldsmith, J. I.; Slinker, J. D.; Rohl, R.; Pascal, R. A., Jr.; Malliaras, G. G.; Bernhard, S. *Chem. Mater.* **2005**, *17*, 5712–5719. (b) Slinker, J. D.; Gorodetsky, A. A.; Lowry, M. S.; Wang, J.; Parker, S.; Rohl, R.; Bernhard, S.; Malliaras, G. G. *J. Am. Chem. Soc.* **2004**, *126*, 2763–2767. (c) Margapoti, E.; Shukla, V.; Valore, A.; Sharma, A.; Dragonetti, C.; Kitts, C. C.; Roberto, D.; Murgia, M.; Ugo, R.; Muccini, M. *J. Phys. Chem. C* **2009**, *113*, 12517–12522. (d) Margapoti, E.; Muccini, M.; Sharma, A.; Colombo, A.; Dragonetti, C.; Roberto, D.; Valore, A. *Dalton Trans.* **2012**, *41*, 9227–9231. (e) Fernandez-Hernandez, J. M.; Yang, C.-H.; Beltran, J. I.; Lemaire, V.; Polo, F.; Frolich, R.; Cornil, J.; De Cola, L. *J. Am. Chem. Soc.* **2011**, *133*, 10543–10558. (f) Zhou, Y.; Han, S.; Zhou, G.; Wong, W.-H.; Roy, V. A. L. *Appl. Phys. Lett.* **2013**, *102*, 083301.
- (5) (a) Baranoff, E.; Yum, J.-H.; Jung, I.; Vulcano, R.; Grätzel, M.; Nazeeruddin, M. K. *Chem.—Asian J.* **2010**, *5*, 496–499. (b) Dragonetti, C.; Valore, A.; Colombo, A.; Righetto, S.; Trifiletti, V. *Inorg. Chim. Acta* **2012**, *388*, 163–167.
- (6) (a) Dragonetti, C.; Righetto, S.; Roberto, D.; Ugo, R.; Valore, A.; Fantacci, S.; Sgamellotti, A.; De Angelis, F. *Chem. Commun.* **2007**, *40*, 4116–4118. (b) Dragonetti, C.; Righetto, S.; Roberto, D.; Ugo, R.; Valore, A.; Demartin, F.; De Angelis, F.; Sgamellotti, A.; Fantacci, S. *Inorg. Chim. Acta* **2008**, *361*, 4070–4076. (c) Dragonetti, C.; Righetto, S.; Roberto, D.; Valore, A.; Benincori, T.; Sannicolò, F.; De Angelis, F.; Fantacci, S. *J. Mater. Sci.: Mater. Electron.* **2009**, *20*, 460–464. (d) Dragonetti, C.; Righetto, S.; Roberto, D.; Valore, A. *Phys. Status Solidi C* **2009**, *6*, S50–S53. (e) Valore, A.; Cariati, E.; Dragonetti, C.; Righetto, S.; Roberto, D.; Ugo, R.; De Angelis, F.; Fantacci, S.; Sgamellotti, A.; Macchioni, A.; Zuccaccia, D. *Chem.—Eur. J.* **2010**, *16*, 4814–4825.
- (7) Aubert, V.; Ordroneau, L.; Escadeillas, M.; Williams, J. A. G.; Boucekkine, A.; Coulaud, E.; Dragonetti, C.; Righetto, S.; Roberto, D.; Ugo, R.; Valore, A.; Singh, A.; Zyss, J.; Ledoux-Rak, I.; Le Bozec, H.; Guerschais, V. *Inorg. Chem.* **2011**, *50*, 5027–5038.
- (8) (a) Levine, B. F.; Bethea, C. G. *Appl. Phys. Lett.* **1974**, *24*, 445–447. (b) Levine, B. F.; Bethea, C. G. *J. Chem. Phys.* **1975**, *63*, 2666–2683. (c) Ledoux, I.; Zyss, J. *Chem. Phys.* **1982**, *73*, 203–213.
- (9) (a) Valore, A.; Colombo, A.; Dragonetti, C.; Righetto, S.; Roberto, D.; Ugo, R.; De Angelis, F.; Fantacci, S. *Chem. Commun.* **2010**, *46*, 2414–2416. (b) Dragonetti, C.; Righetto, S.; Roberto, D.; Ugo, R.; Valore, A.; Ledoux-Rak, I. *Nonlinear Opt., Quantum Opt.* **2012**, *43*, 197.
- (10) Zaarour, M.; Guerschais, V.; Le Bozec, H.; Dragonetti, C.; Righetto, S.; Roberto, D.; De Angelis, F.; Fantacci, S.; Lobello, M. G. *Dalton Trans.* **2013**, *42*, 155–159.
- (11) Tamayo, A. B.; Alleyne, B. D.; Djurovich, P. I.; Lamansky, S.; Tsyba, I.; Ho, N. N.; Bau, R.; Thompson, M. E. *J. Am. Chem. Soc.* **2003**, *125*, 7377–7387.
- (12) Lamigni, L.; Barbieri, A.; Sabatini, C.; Ventura, B.; Barigelletti, F. *Top. Curr. Chem.* **2007**, *281*, 143–203.
- (13) King, K. A.; Spellane, P. J.; Watts, R. J. *J. Am. Chem. Soc.* **1985**, *107*, 1431–1432.
- (14) Fery-Forgues, S.; Delavaux-Nicot, B. *J. Photochem. Photobiol., A* **2000**, *132*, 137–159.
- (15) (a) Xia, X. B.; Ding, Z. F.; Liu, J. Z. *J. Photochem. Photobiol., A* **1995**, *88*, 81–84. (b) Li, Y.; Qi, H.; Peng, Y.; Gao, Q.; Zhang, C. *Electrochem. Commun.* **2008**, *10*, 1322–1325. (c) Siemeling, U.; Bausch, K.; Fink, H.; Bruhn, C.; Baldus, M.; Angerstein, B.; Plessow, R.; Brockhinke, A. *Dalton Trans.* **2005**, 2365–2374.
- (16) Roberto, D.; Colombo, A.; Locatelli, D.; Tessore, F.; Ugo, R.; Cavazzini, M.; Quici, S.; De Angelis, F.; Fantacci, S.; Ledoux-Rak, I.; Tancrez, N.; Zyss, J. *Dalton Trans.* **2012**, *41*, 6707–6714.
- (17) Brey, J.; Stössel, P.; Schrader, S.; Starukhin, A.; Finkenzeller, W. J.; Yersin, H. *Chem. Mater.* **2005**, *17*, 1745–1752.
- (18) Kanis, D. R.; Lacroix, P. G.; Ratner, M. A.; Marks, T. J. *J. Am. Chem. Soc.* **1994**, *116*, 10089–10102.
- (19) (a) Maker, P. D. *Phys. Rev. A* **1970**, *1*, 923–951. (b) Zyss, J. *J. Chem. Phys.* **1993**, *98*, 6583–6600. (c) Clays, K.; Persoons, A. *Phys. Rev. Lett.* **1991**, *66*, 2980–2983. (d) Zyss, J.; Ledoux, I. *Chem. Rev.* **1994**, *94*, 77–105.
- (20) Maury, O.; Viau, L.; Sénéchal, K.; Corre, B.; Guégan, J.-P.; Renouard, T.; Ledoux, I.; Zyss, J.; Le Bozec, H. *Chem.—Eur. J.* **2004**, *10*, 4454–4466.
- (21) Claessens, C. G.; Gonzalez-Rodriguez, D.; Torres, T.; Martin, G.; Agullo-Lopez, F.; Ledoux, I.; Zyss, J.; Ferro, V. R.; Garcia de la Vega, J. M. *J. Phys. Chem. B* **2005**, *109*, 3800–3809.
- (22) Prim, D.; Kirsch, G.; Nicoud, J. F. *Synlett* **1998**, *4*, 383–384.
- (23) Dumur, F.; Mayer, C. R.; Dumas, E.; Miomandre, F.; Frigoli, M.; Sécheresse, F. *Org. Lett.* **2008**, *10*, 321–324.
- (24) (a) Adamo, C.; Barone, V. *J. Chem. Phys.* **1999**, *110*, 6158–6170. (b) Ernzerhof, M.; Scuseria, G. E. *J. Chem. Phys.* **1999**, *110*, 5029–5036. (c) Kadari, A.; Moncomble, A.; Ciofini, I.; Brahim, M.; Adamo, C. *J. Phys. Chem. A* **2011**, *115*, 11861–11865.
- (25) Hay, P. J.; Wadt, W. R. *J. Chem. Phys.* **1985**, *82*, 270–283, 299–310.
- (26) Frisch, M. J.; Trucks, G. W.; Schlegel, H. B.; Scuseria, G. E.; Robb, M. A.; Cheeseman, J. R.; Scalmani, G.; Barone, V.; Mennucci, B.; Petersson, G. A.; Nakatsuji, H.; Caricato, M.; Li, X.; Hratchian, H. P.; Izmaylov, A. F.; Bloino, J.; Zheng, G.; Sonnenberg, J. L.; Hada, M.; Ehara, M.; Toyota, K.; Fukuda, R.; Hasegawa, J.; Ishida, M.; Nakajima, T.; Honda, Y.; Kitao, O.; Nakai, H.; Vreven, T.; Montgomery, J. A., Jr.; Peralta, J. E.; Ogliaro, F.; Bearpark, M.; Heyd, J. J.; Brothers, E.; Kudin, K. N.; Staroverov, V. N.; Kobayashi, R.; Normand, J.; Raghavachari, K.; Rendell, A.; Burant, J. C.; Iyengar, S. S.; Tomasi, J.; Cossi, M.; Rega, N.; Millam, J. M.; Klene, M.; Knox, J. E.; Cross, J. B.; Bakken, V.; Adamo, C.; Jaramillo, J.; Gomperts, R.; Stratmann, R. E.; Yazyev, O.; Austin, A. J.; Cammi, R.; Pomelli, C.; Ochterski, J. W.; Martin, R. L.; Morokuma, K.; Zakrzewski, V. G.; Voth, G. A.; Salvador, P.; Dannenberg, J. J.; Dapprich, S.; Daniels, A. D.; Farkas, O.; Foresman, J. B.; Ortiz, J. V.; Cioslowski, J.; Fox, D. J. *Gaussian 09*, revision A.02; Gaussian, Inc.: Wallingford, CT, 2009.
- (27) Flükiger, P.; Lüthi, H. P.; Portmann, S.; Weber, J. *Molekel 4.3*; Swiss Center for Scientific Computing: Manno, Switzerland, 2000–2002.